JOURNAL OF THE KOREAN ASTRONOMICAL SOCIETY
36: 43 ~ 48, 2003

PERFORMANCE OF THE SRAO 6-METER RADIO TELESCOPE

BON-CHUL KOO, YONG-SUN PARK, SEUNG SOO HONG, HONG-SIK YUN, SANG-GAK LEE,
DO-YOUNG BYUN, JUNG-WON LEE, HAN-KYU CHOI, SANG-SUNG LEE, YOUNG-ZOO YOON,

KEE-TAE KIM*, HYUN WOO KANG, AND JUNG-EUN LEE†
Astronomy Program, SEES, Seoul National University, Seoul 151-747, Korea
E-mail: koo@astrohi.snu.ac.kr
(Received Mar. 12, 2003; Accepted Mar. 24, 2003)

ABSTRACT

We introduce and describe performance of the 6-meter telescope of Seoul Radio Astronomy Observatory (SRAO). All the softwares and instruments except the antenna structure and its driving system are developed for ourselves. The SIS mixer type receiver resulted in the receiver noise temperature less than 50 K (DSB) over the whole 3-mm radio window. An autocorrelation spectrometer, developed first in Korea, provides maximum 50 MHz band width over 1024 channels. Antenna surface is measured and adjusted using template method and radio holography which resulted in a superb surface accuracy better than $30\mu m$. Accordingly, the aperture and beam efficiences amount to 70 % and 75 %, respectively, largely independent of frequency in the 85 – 115 GHz range. It is also found that telescope pointing errors are less than $10''$ in both azimuth and elevation and that antenna gain is almost constant against elevation greater than 20°, without adjusting sub-reflector position. The SRAO 6-meter telescope is now fully operational and all these characteristics verify that observations are carried out with high precision and fidelity.

Key words : instruments:radio telescope

I. INTRODUCTION

A new 6-meter radio telescope, the second millimeter wave radio telescope in Korea, is inaugurated for the astronomy community. The telescope is located in the campus of Seoul National University (Fig. 1), and its regular observations started from October, 2001. Hereby we introduce the SRAO telescope and describe its general features and performance.

Antenna structure and driving system were made by Minex corp., USA. All other instruments including receiver and spectrometer were built for ourselves. We also developed softwares for telescope control and data acquisition. Given are performances of the receiver system and the autocorrelation spectrometer.

Main reflector consisting of 84 smaller panels has been adjusted first with a swing template and then using radio holography, to conform to a predetermined paraboloidal shape as accurately as possible. We confirm the superb surface accuracy of main reflector by observing celestial standard radio source. Finally, the pointing accuracy and elevation dependence of antenna gain are investigated and discussed.

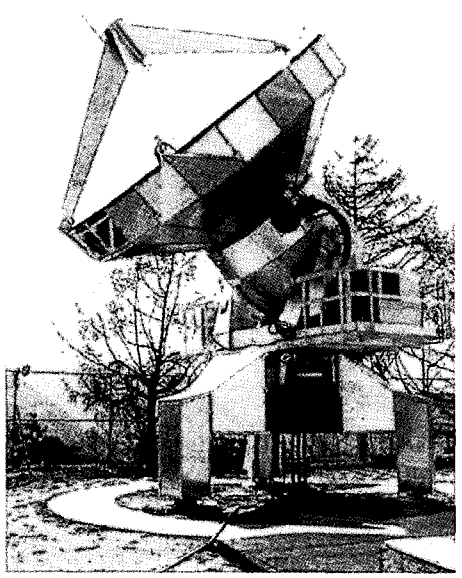

Fig. 1.— Photo of the SRAO 6-meter telescope.

Corresponding Author: B.-C. Koo

*currently at University of Illinois at Urbana-Champaign, USA

†now at University of Texas at Austin, USA

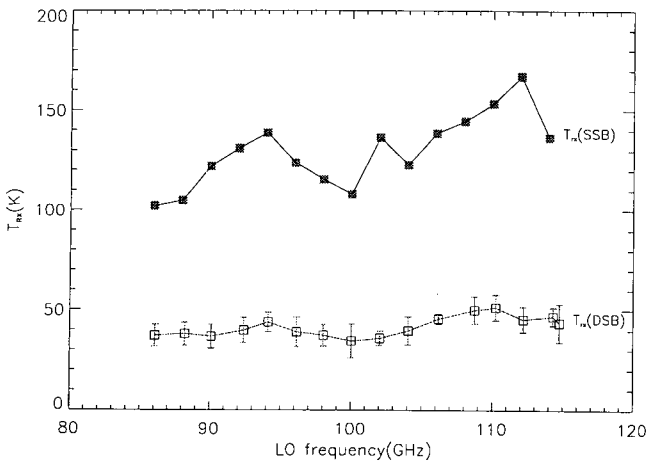

Fig. 2.— The noise temperature of the SIS receiver (Lee et al. 2002).

II. CONTRUCTION OF HARDWARES

(a) Antenna

The antenna is 6.1 meter in diameter, and the effective focal ratio of main and sub-reflector is 4.69, while the f/D ratio of the main reflector itself is 0.42 (Hudson 1998). The hyperbolic sub-reflector is 61 cm in diameter and is supported by three legs. The main dish is composed of 84 aluminum panels, with the surface accuracy of individual panel of $\sim 5\mu$m. The panels as a whole should form a paraboloid specified by the focal length of the main reflector to an accuracy of at least $\lambda/20$. In the first phase, the panels were adjusted by using a template that swings with respect to the symmetry axis. Its profile defines the paraboloidal shape of the antenna. The best accuracy that can be obtained with this method is known to be around 100μm. From the observation of Venus, we found that the surface accuracy was $120 - 150\mu$m and that the aperture and beam efficiencies were 54 % and 56 %, respectively, at around 100 GHz. In the second phase, we adopted radio holographic method to pursue much better measurement accuracy, which will be detailed in section IV.

(b) Receiver

A heterodyne type receiver is designed and developed using the SIS junction. The junction is kindly provided by Nobeyama Radio Observatory, Japan, via Taeduk Radio Astronomy Observatory. Input frequency range is 85 – 115 GHz and the IF (intermediate frequency) is 1.5 GHz with an instantaneous bandwidth of 400 MHz. A scalar feed horn, an SIS mixer, and a first stage IF amplifier are cooled down to 4.5 K in a vacuum dewar. Quasi-optical part composed of ellipsoidal mirrors and SSB (single side band) filter is located between the sub-reflector and horn, which rejects image band and provides 12-dB illumination of the horn onto the sub-reflector.

The measured receiver temperature is found to be less than 50 K in DSB (double side band) over the whole input frequency range as shown in Figure 2. The SSB receiver temperature is around 130 K, more than twice of the DSB receiver temperature, due to the noise contribution from the SSB filter and image termination. This performance stands comparison with those of other observatories in the world. Detailed description of the receiver system is given elsewhere (Lee et al. 2002). The SSB system temperature is found to be less than 200 K for 85 – 100 GHz and 500 K for 115 GHz at the best weather condition in winter.

(c) Autocorrelation Spectrometer

The design goal is to develop an autocorrelation spectrometer with a maximum bandwidth of 50 MHz and the number of channels of 1024. For this, hardware based on high speed digital technology is designed to perform three levels and Nyquist sampling. A correlator chip conducts the calculations of auto-correlation function and a PC carries out numerical Fourier transformation. The performance of the autocorrelator was verified by comparing profiles of molecular lines from celestial objects with those obtained with a filter bank. They are found to be identical within observational accuracy. Details are described in a separate paper (Choe, Byun & Koo 2003).

III. SOFTWARE DEVELOPMENT

Following the current trend of using low cost PCs as platforms of telescope control and others, three PCs are used for source tracking, data taking, and data processing. In order to guarantee high fidelity, we adopt Linux for OS. All the subsequent development of programs are based on this OS and implemented using C and C++ programming language. We design the control programs in such a way that modular and multiprocess structure can be achieved as much as possible for easy debugging and upgrading. Command streams between processes on different PCs are sent through ethernet lines using TCP/IP socket. When very fast responses are necessay, we use parallel bit I/O lines which directly connect the PCs.

Antenna control is one of the most important part of the control system and we use a motion control card with a micro-controller. Main computer calculates the position and velocity of an object in horizontal coordinate and sends them to the motion control card at intervals of three seconds. Then the process running on the micro-controller adjusts the output pulse train that is fed into driving motors. The frequency of output pulses is updated with the period of 30 milliseconds. The measured antenna tracking accuracy is found to be better than $0.4''$.

An accurate time standard is necessary for source tracking. We synchronize the system time using Net-

work Time Protocall. The accuracy is about 20 milliseconds, which is much better than the allowed tolerance of 300 milliseconds.

We prepare two observation modes: in an interactive mode, an observer inputs parameters via Graphic User Interface while carrying out observations. The other is called a schedule mode that an observer prepares a text file containing his observing plan and submits it before observation. Data are finally converted to files that are compatible with a popular data reduction package, CLASS. Details of the software system will be described in a forthcoming paper (Byun et al. 2003).

IV. EFFICIENCY MEASUREMENTS

(a) Holographic Surface Measurements

To achieve better rate of data production and to open a new radio window up to 270 GHz in near future, we need to upgrade the antenna surface at least down to 50μm. In the second phase after applying the swing template method mentioned in section II, we decided to adopt the 'with-phase' holography to measure and correct the main reflector surface. By 'with-phase' we mean that a *complex* beam pattern is measured and Fourier transformed to yield aperture distribution (Scott & Ryle 1977). The phase of the aperture distribution contains information on the deviation of panels with respect to an ideal paraboloid, whereas the amplitude, the degree of illumination of the receiver system onto the sub-reflector.

In order to measure the complex beam pattern, one needs signal source that is either in far field (i.e., celestial radio source or satellite) or in near field (e.g., transmitter on a mountain top). Moreover, one additional antenna and receiver are necessary to provide a reference in measuring the phase. Among diverse holography methods, the 'with-phase' holography together with a transmitter guarantees the best signal-to-noise ratio.

We first set a transmitter at the top of Kwanak mountain and placed a reference antenna in the vicinity of the SRAO 6-meter antenna under test. One of the drawbacks in using transmitter is that it is usually in near field just like this experiment. However, the near field effect can be easily corrected, if the distance between transmitter and receiver (i.e., antenna under test) is known with reasonable accuracy (Zhang 1996; Zhang et al. 1996). Experience says that even this correction may not be necessary, since the deviation of aperture distribution due to being in the near field is functionally similar to that due to defocus effect, which can be easily identified.

Making use of harmonic mixers to reduce cost and of microwave instruments available in the laboratory, we made receivers for two antennae to catch the signal at 86 GHz from the transmitter. Signals from two antennae are down-converted and cross-correlated to derive amplitude and phase of the beam pattern. Then Fourier transformation is performed, and after correcting large scale deformation, aperture distribution is finally determined. Details of the experiment will be described in a forthcoming paper (Lee et al. 2003).

Figure 3 shows the surface structure before and after several measurements and adjustments of the panels. The structure before the adjustments is regarded as the status just after applying the swing template method. One can notice ring structure which is a natural consequence of using the swing template. The surface accuracy is drastically improved from $\sim 100\mu$m to $\sim 30\mu$m after holographic adjustments. The value of $\sim 100\mu$m is roughly coincident with the one derived in section II. The final value of $\sim 30\mu$m is good enough to enable observations up to 300 GHz.

Concomitantly, we can derive edge taper by using the amplitude distribution in the main reflector. The edge taper is found to be around 11 dB, which is very close to the design value of 12 dB. Although we used most of the quasi-optical components as they were, the location of the feed horn has been changed for the correction of near field. This may be one of the reasons for the small discrepancy.

(b) Beam Size

The superb surface accuracy should be verified by the greatly improved aperture and beam efficiencies. Those efficiencies can be estimated by observing calibration sources like planets. Since a planet can be approximated as disk with uniform brightness, the measured antenna temperature, T_A^*, is related to the aperture (η_A) and beam (η_B) efficiency in the following way (Roh & Jung 1999).

$$\eta_A \equiv \frac{A_e}{A_p} = \frac{\lambda^2 T_A^*}{A_p T_B \Omega_s}, \tag{1}$$

$$\eta_B \equiv \frac{\Omega_s}{\Omega_A} = \frac{T_A^* \Omega_M}{T_B \Omega_s}, \tag{2}$$

$$\Omega_s = \Omega_M [1 - \exp(-\ln 2 (\frac{\theta_s}{\theta_M})^2)], \tag{3}$$

$$\Omega_M = 1.133 \theta_M^2. \tag{4}$$

We have cross-scanned the Orion KL in the SiO maser line in order to measure beam size, θ_M. From several scans both in AZ and EL directions that are shown in Figure 4, we get $\theta_M = 130'' \pm 3''$ at 86 GHz. The difference between AZ and EL directions are less than 2 %. Theoretical calculation shows that

$$\theta_M = [1.02 + 0.0135 T_e(\mathrm{dB})] \frac{\lambda}{D}, \tag{5}$$

where D is antenna diameter and T_e is the edge taper (Goldsmith 1998). It is found that the observed beam size is smaller than the theoretical one, 138″, for 11 dB edge taper. For other frequencies, it is assumed that

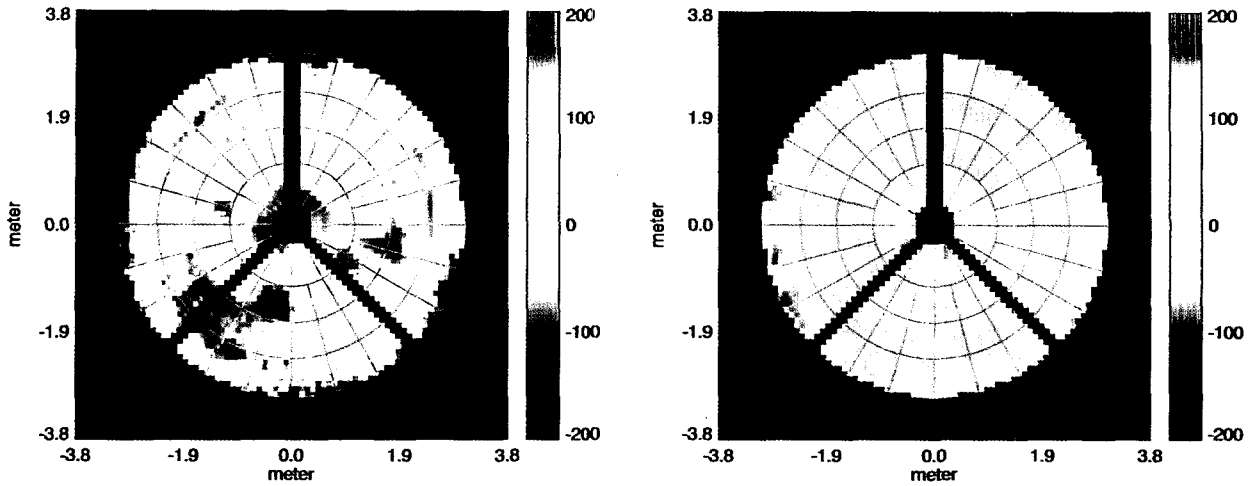

Fig. 3.— Surface structure before (*left*) and after (*right*) adjustments by holographic experiment. The surface accuracy is improved from $\sim 100\mu$m to $\sim 30\mu$m. The spatial resolution of the measurements is 10cm x 10cm. The reversed Y shape is the shadow of spar supporting the sub-reflector. A black square in the lower part of the figure on the left is an artifact by a teflon sheet which was overlaid on the antenna surface to test the sensitivity of the experiment. The size of the teflon sheet is 50cm x 50cm and its thickness is 1 mm. Since the teflon sheet has an index of refraction of 1.4, the area covered by the sheet looks as if it is sunk down by 400μm.

θ_M is proportional to wavelength. The beam size is summarized in Table 1.

In order to verify the beam size at other frequencies, we have mapped Venus in three frequencies of 86.2, 100, and 110 GHz, when it is close to Earth in Nov. 2002. Since the measured beam size is a convolution of disk and Gaussian beam, one needs to deconvolve the image in order to derive the true beam size. Since the beam size is greater than 100″, while the angular size of Venus is 40″ – 50″, the amount of correction is not so large. Using the correction table in Minh (1994), we derive the beam size of 127″, 108″, and 104″, for 86.2, 100, and 110 GHz, respectively. It is found that the beam size is rather dependent on the scanning direction. These values are thus the average of them in both directions. After discarding the noisy 110 GHz data, we find that the beam size derived in this way is even smaller than the previous ones. However, the difference between two measurements is only a few percents. Thus we use the beam size derived from the SiO observation and scaled to other wavelength, since the continuum observation of Venus is more subject to the power fluctuations of the receiver system, resulting in larger observational uncertainty.

(c) Aperture and Beam Efficiencies

Then the aperture and beam efficiencies can be readily calculated by using equations (1) through (4) with the brightness temperature of Venus taken from Ulich

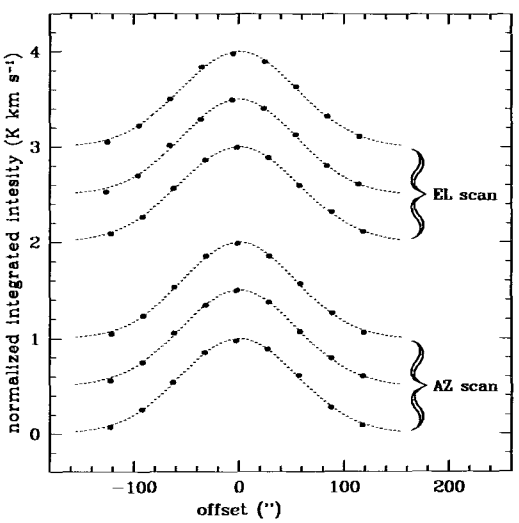

Fig. 4.— Cross scan maps of Orion KL in SiO maser line at 86.2 GHz (dots). Gauss fitting curves are shown together (dashed lines).

(1981). The resulting aperture and beam efficiency amounts to 70 % and 75 %, respectively (Table 1). Both efficiencies are largely independent of frequency, as is expected if the surface accuracy is very high. This efficiency is very close to that of BIMA (Berkeley-Illinois-Maryland Association) whose surface accuracy is claimed to be $\lesssim 30\mu$m (http://astro.bima.umd.edu/). This is suggestive since the SRAO antenna is identical to that of BIMA. Actually the aperture efficiency is related to the surface accuracy as follows:

$$\eta_A = \eta_{A_0} \exp[-(\frac{4\pi\sigma}{\lambda})^2]. \quad (6)$$

Therefore one can derive the surface accuracy, σ, in principle. However, a difficulty arises from the fact that η_{A_0} remains largely uncertain. Considering the edge taper of $\sim$ 12 dB only, the η_{A_0} will be $\sim$ 0.80 (Goldsmith 1998). Other factors like the shadowing of sub-reflector and spar may make η_{A_0} close to 0.75 (Lugten 1995). Then the surface accuracy of $\lesssim 30\mu$m can be verified. The more accurate estimation will be available when the 230 GHz receiver is operational.

The aperture and beam efficiencies are used for the absolute calibration of point radio sources and of sources presumably filling just the main beam of the telescope, respectively. For more extended objects, which are more common, forward spillover and scattering efficiency, η_{fss}, is more favorable. It is often replaced by η_{moon}, a fraction of beam response subtending the moon's angular size, i.e.,

$$\eta_{moon} \equiv \frac{T_A^*(moon)}{T_b(moon)}. \quad (7)$$

The brightness temperature of the Moon depends on the phase, ϕ, as follows:

$$T_b(moon) = 235[1 + \frac{0.77}{\sqrt{1+2\Delta+2\Delta^2}} \cos(\phi - \arctan\frac{\Delta}{1+\Delta})], \quad (8)$$

where $\Delta = 0.3\lambda$, T_b is in K, and λ in mm (Roh & Jung 1999).

We observed the Moon when $\phi \approx 225°$, early Jan. 2003. Since the measured brightness is found to be not so uniform across the surface, we averaged the antenna temperature toward the central disk with a radius of 8′.

Table 1 summarizes the measured aperture and beam efficiencies, and the moon efficiency for three frequencies. These pieces of information should be used in calibrating radio data and in deriving physical quantities like flux or brightness temperature.

V. MEASUREMENTS OF POINTING ACCURACY AND ANTENNA GAIN VARIATION

The tracking accuracy is better than 0.4″ as mentioned in section II. However, even though telescope faithfully tracks celestial objects according to the command from computer, it does not necessarily mean that the telescope points the celestial objects exactly, since there are many sources of pointing errors like the tilt of telescope base, non-orthogonality of AZ and EL axes, and non-collimation between beam axis and mechanical axis. These pointing errors are not random, but have a functional form. It can be corrected by monitoring *optically* identified radio sources such as planets and SiO maser sources.

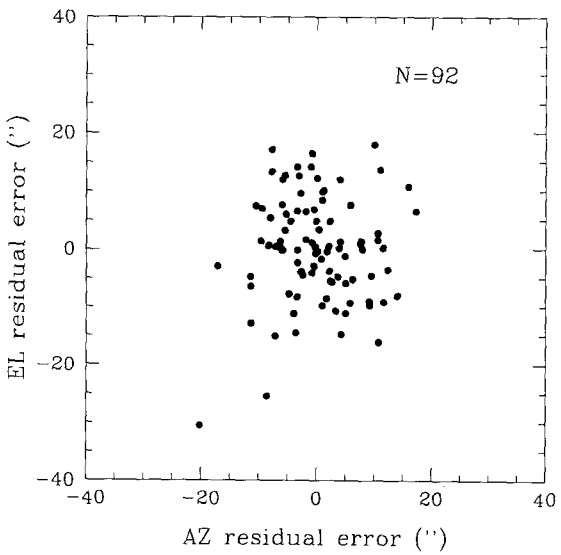

Fig. 5.— Distribution of residual pointing errors in both AZ and EL directions. The σ's are 9″ and 7″ for AZ and EL directions, respectively.

Observation for pointing correction is carried out typically once a year before each observing season. Figure 5 shows the distribution of residual errors after removing terms mentioned above, which is obtained just before this season. The final pointing accuracy is estimated to be $\sigma \lesssim 10''$ in both directions of AZ and EL. It is often found that the pointing error changes drastically (max. 30″) between day and night time. This may be caused by the different illumination of sunlight on the antenna structure. Although the antenna structure is covered by sun shade and fans circulate air in the back side of antenna, sub-reflector, and spar, they don't seem to work enough to keep the temperature uniform. This may be of a serious problem when the 230 GHz band observation gets started.

How much degree the antenna is deformed due to gravitation is of another concern. Since most radio sources do not change brightness during observation, gain variation can be easily tested by observing any objects for a range of elevation. Since this effect will be the most prominent for point source, we observed an SiO source, Orion KL. We found actually no variation

Table 1. Beam Size and Various Efficiencies

frequency (GHz)	θ_M ($''$)	$\theta_M/(\lambda/D)$	η_A (%)	η_B (%)	η_{moon} (%)
86.2	130 ± 3	1.10	71 ± 6	77 ± 7	92 ± 2
100	112 ± 2	1.10	72 ± 3	78 ± 3	88 ± 3
110	101 ± 2	1.10	69 ± 5	73 ± 6	88 ± 3

against elevation greater than 20°. It should be also noted that, during this observation, we did not adjust sub-reflector position which is usually done in other telescopes. Since SRAO 6-meter telescope is rather small sized and originally designed for interferometer use, the structure is quite stiff. This will be the explanation for constant antenna gain over a wide range of elevation. It is concluded that the SRAO telescope is stiff enough, and thus provides constant antenna gain for EL $\gtrsim$ 20°.

VI. SUMMARY

The general features of the SRAO 6-meter radio telescope are reviewed, that was completed a couple of years ago and is now under regular operation.

All the equipments except the antenna structure and driving system were made by SRAO staff. The average DSB receiver temperature of 50 K over 3 mm band is comparable to those of other radio observatories in the world. We also made an autocorrelation spectrometer with a maximum band width of 50 MHz for the first time in Korea. Softwares for source tracking, data acquisition, and antenna control, were developed based on the Linux OS with popular PCs.

Main reflector surface was measured and adjusted by employing the swing template method and radio holography, which resulted in the surface accuracy of $\sim 30\mu$m or $\lambda/40$ at 230 GHz. Consequently, aperture and beam efficiencies are found to be $\sim$ 70 % and $\sim$ 75 %, respectively, being nearly constant over the $85-115$ GHz band.

It is also found that pointing accuracy is better than one tenth of beam size and that antenna gain is constant over a wide range of elevation without the adjustment of sub-reflector position.

All these characteristics of the SRAO 6-meter telescope enable the production of reliable radio data.

ACKNOWLEDGEMENTS

The SRAO 6-m telescope project would have not succeeded without the supports from many people. First of all we wish to thank Carl Heiles, Leo Blitz, Jack Welch, Matt Fleming, and many people at Berkeley Radio Astronomy Lab for their generous support for getting the antenna system. We thank Jae-Hoon Jung, Seog-Tae Han, Kwang-Dong Kim, Jong-Ae Park, Tae-Seong Kim, and many people at TRAO for their unselfish supports for building the receiver system. We thank Ray Escoffier and people at NRAO for their highly technical supports in making the spectrometer. We also thank Pil-Ho Park, Jeong-Ho Joh, and Jong-Uk Park at KAO for measuring the precise coordinate of the SRAO position. Se-Hyung Cho at KAO and Young Key Minn at KHU gave us invaluable advices and supports. Finally we thank the faculty members and graduate students at the SNU Astronomy Department for their well coordinated supports over the entire period of the project. This study is supported by Seoul National University, Ministry of Education, and Ministry of Science and Technology, Korea, via grant 00-N-A5-01-A-02 and KISTEP program M1-0222-00-0007.

REFERENCES

Byun, D.-Y. et al., 2003, in preparation

Choi, H.K., Byun, D.-Y., Koo, B.-C., 2003, International Journal of Infrared and Millimeter Waves, in press

Goldsmith, P.F., Quasioptical Systems, 1998, IEEE Press

Hudson, J.A., 1998, "Ray-tracing the BIMA Reflectors", BIMA memo, No. 64

Korea Astronomy Observatory, Korean Astronomical Almanac, 2002

Lee, J.W., Han, S.T., Byun, D.-Y., Koo, B.-C., Park, Y.-S., 2002, "Development of SRAO 3 MM SIS receiver", International Journal of Infrared and Millimeter waves, 23, 47

Lee, S.S. et al., 2003, in preparation

Lugten, J., 1995, "Optical Design and Performance of the BIMA Interferometer", BIMA memo, No. 39

Minh, Y.C., 1994, Radio Astronomy, DongYang Press

Scott, P.F., Ryle, M., 1977, "A rapid method for measuring the figure of a radio telescope reflector", MNRAS, 178, 539

Roh, D.G., Jung, J.H., 1999, "Characteristics of TRAO 14m Radio Telescope (1999)", Publications of Korean Astronomical Society, 14, 123

Ulich, B.L., 1981, "Millimeter-wavelength continuum calibration sources", ApJ, 86, 1619

Zhang, X., 1996, "Certain Optics Considerations for the Holography Experiment", SMA technical memo, No. 86

Zhang, X., Levine, M., Brakto, P., Test, J., Papa, C., Masson, C., 1996, "Planned Panel Adjustment Procedure for SMA Antennae Using the Microwave Holography Technique", SMA technical memo, No. 85